Applied Catalysis A, General 565 (2018) 152–162

Contents lists available at ScienceDirect

Applied Catalysis A, General

journal homepage: www.elsevier.com/locate/apcata

CO oxidation over Co-catalysts supported on silica-titania – The effects of the catalyst preparation method and the amount of incorporated Ti on the formation of more active Co^{3+} species

Thiago M. Lima[a,e], William N. Castelblanco[a], Ariano D. Rodrigues[b], Rodolfo E. Roncolatto[c], Leandro Martins[d], Ernesto A. Urquieta-González[a,*]

[a] Research Center on Advanced Materials and Energy, São Carlos Federal University, C. Postal 676, 13565-905, São Carlos, SP, Brazil
[b] Department of Physics, São Carlos Federal University, C. Postal 676, CEP 3565-905, São Carlos, SP, Brazil
[c] Cenpes/Petrobras, Av. Horácio Macedo 950, Ilha do Fundão, Rio de Janeiro, RJ, Brazil
[d] Instituto de Química, UNESP - Univ. Estadual Paulista, Rua Prof. Francisco Degni 55, CEP 14800-900, Araraquara, SP, Brazil
[e] Departamento de Química Inorgânica, Universidade Federal Fluminense, Campus do Valonguinho, Outeiro São João Batista s/n, Centro, 24020-150 Niterói, RJ, Brazil

ARTICLE INFO

Keywords:
Cobalt oxide
Silica
Titania
Silica-titania
CO oxidation
One-pot methodology

ABSTRACT

Herein, a sol-gel one-pot methodology to tune the activity of Co-catalysts supported on silica-titania to CO oxidation is described. SEM, TEM, EDS, XPS and H_2-TPR evidenced a higher Co dispersion from that method when compared to catalysts prepared by impregnation. Furthermore, the simultaneous addition of cobalt oxalate during the incorporation by sol-gel of a controlled low Ti amount into the silica (Si/Ti = 5.7) was determinant to improve the Co dispersion and to avoid the formation of Co-species with strong support interaction. Moreover, XPS analyses evidenced that the mentioned low Ti amount favoured a higher formation of superficial Co^{3+} and lattice O^{2-} species, which promoted a higher CO oxidation specific activity and, more importantly, strongly decreasing the light-off temperature. On the other hand, Rietveld analyses, Raman spectroscopy, H_2-TPR and XPS data showed that the incorporation of higher amounts of Ti into the silica (Si/Ti = 0.2) led to the formation of cobalt titanate, decreasing the concentration of superficial Co^{3+} and lattice O^{2-} species and, consequently, decreasing the specific activity toCO oxidation.

1. Introduction

In the last years, the growing use of fossil fuels burned in transportation systems, power plants and domestic necessities has led to an alarming worldwide increase in the concentration carbon monoxide (CO) in the atmosphere. Since CO is a dangerous pollutant owing to its high affinity with hemoglobin, which leads to the formation of carboxyhemoglobin compromising oxygen transport and being lethal in concentrations above of 650 ppm, studies on this gas have considerably grown in recent times [1].

In this context, the heterogeneous catalytic oxidation of CO is currently the most effective approach for its abatement, and the commercial catalysts to this end are mostly based on noble metals, as a consequence of their high activity for CO oxidation and stability [2–7]. However, it is well-known that the major drawback in the use of noble metals is related to their scarcity and high and increasing cost [1,8]. Consequently, several studies have been reported on the development of non-noble transition metal-based catalysts for CO oxidation. [1,9–14] Cobalt oxides, Co_3O_4 especially, present excellent activity in said reaction as a consequence of the capability of oxygen uptaking in their lattice structure; additionally, they readily undergo redox reactions in which pair $Co^{2+} \leftrightarrow Co^{3+}$ deeply participates in the reaction through the adsorption of the CO and O_2 reactant molecules. Furthermore, several reports in the literature discuss the great importance of the Co^{3+} cation in the process, since this species is the most active one for the CO adsorption and oxidation, whereas the Co^{2+} species possess a lower activity [15,16]. The CO oxidation mechanism over Co_3O_4 involves four fundamental steps, which are: (i) CO adsorption, (ii) reaction between the adsorbed CO and a lattice oxygen from Co_3O_4, forming an adsorbed CO_2 molecule, (iii) CO_2 desorption, (iv) adsorption of an oxygen molecule, restoring the oxidation state of the active site and lattice oxygen [17].

Several studies have been reported on the synthesis of highly active unsupported cobalt oxide catalysts for CO oxidation, for instance Co_3O_4

* Corresponding author.
E-mail address: urquieta@ufscar.br (E.A. Urquieta-González).

https://doi.org/10.1016/j.apcata.2018.08.006
Received 18 May 2018; Received in revised form 8 August 2018; Accepted 9 August 2018
Available online 10 August 2018
0926-860X/

nanorods with preferential exposure of Co^{3+} cations, Co_3O_4 nanoparticles with different shapes and sizes and mesoporous Co_3O_4 with ordered mesopores [18–21]. However, unsupported transition metal oxides tend to deactivate at higher temperatures due to nanoparticles sintering [22]. Despite the scientific importance of the discussed studies, the use of such unsupported cobalt oxides as catalysts for the abatement of pollutants in exhaust systems of industrial plants or where the processes are operated under severe conditions seems to be infeasible. In this context, the preparation of supported transition metal oxides is highly desirable for such applications.

Thus, the catalyst support could play a crucial role in the dispersion of the active phase and, in this sense, supports constituted by oxides have been considered promising on account of their tunable physicochemical and textural features [23]. More specifically, the SiO_2-TiO_2 system has attracted much attention as a support [23] in reactions such as CO hydrogenation [24], SCR of NO with NH_3, and NO reduction with CO [25]. Most of the cited authors have claimed that silica-titania promote the generation of new active sites arising from the interaction between them, also enhancing the thermal and mechanical stabilities of the final catalyst [26].

Furthermore, the development of greener procedures for the synthesis of supported catalysts is necessary in order to minimize the generation of chemical waste, catalyst cost and energy consumption. Thus, the one-pot synthesis of catalysts emerges as a promising approach for heterogeneous catalysts preparation [27].

To the best of our knowledge, the use of Co-catalysts supported on SiO_2-TiO_2 has not yet been reported for CO oxidation, which opens a window of opportunities regarding the potential use of these catalysts for environmental applications. With those concepts in mind, herein we report the preparation of Co_3O_4 supported on silica-titania by a sol-gel one-pot methodology introducing cobalt oxalate - the cobalt oxide precursor salt - into the synthesis mixture of the support and their application as potential CO oxidation catalysts with tunable specific activities. For comparison purposes, Co-catalysts were also prepared by conventional impregnation with a cobalt nitrate solution, since this method is commonly employed at industrial level. The obtained cobalt catalysts with different titanium amounts incorporated into the silica support were characterized by inductively coupled plasma mass spectrometry (ICP-MS), energy dispersive X-ray fluorescence (EDS-XRF), X-ray diffraction (XRD), nitrogen adsorption/desorption measurements, temperature programmed reduction with hydrogen (H_2-TPR), Raman and X-ray photoelectron (XPS) spectroscopies, scanning and transmission electron microscopies with simultaneos chemical analysis by energy dispersive X-ray (SEM-EDS and TEM-EDS, respectively). The prepared cobalt catalysts had their activity evaluated in the CO oxidation reaction.

2. Experimental

2.1. Synthesis of the pure supports

The pure supports were synthesized by a sol-gel approach as described by Wang et al. [28] SiO_2-TiO_2 supports (named as ST) were prepared using the triblock copolymer $EO_{20}PO_{70}EO_{20}$ (Pluronic®P123) as a structural agent, aiming the formation of mesopores [28]. Tetraethyl orthosilicate (TEOS) and titanium tetraisopropoxide (TTIP) were the sources of silicon and titanium, respectively, and acetylacetone (ACAC) was used as a complexing agent to prevent the fast hydrolysis of the TTIP. Thus, 3.2 g of the surfactant Pluronic®P123 were dissolved in a solution containing 60 mL of sodium acetate-acid acetic buffer (pH = 5.0, $[C_t] = 0.02\ mol\ L^{-1}$) and 3.4 mL of a Na_2SO_4 solution ($0.4\ mol\ L^{-1}$) at 50 °C. After the complete dissolution of the surfactant, 4.4 mL of TEOS were added under vigorous stirring followed by the addition of a predetermined amount of TTIP mixed with ACAC. The added amount of titanium alkoxide was calculated to obtain three different nominal Si/Ti molar ratios: 5.7, 1.0 and 0.2, corresponding to Ti weight fractions (wt.%) of 15, 50 and 85%, respectively. In all the syntheses, the Ti and ACAC molar ratio was kept equal to 2. Then, the stirring was stopped and the mixture left under static conditions for 24 h and then refluxed at 100 °C for another 24 h. The obtained gel was separated by filtration and then washed several times with distilled water, followed by drying at 80 °C for 24 h and finally calcination at 550 °C for 5 h (heating rate of $5\ °C\ min^{-1}$). The silica (named as S) and titania (named as T) pure supports were also prepared according to the same described methodology.

Table 1
Si/Ti molar ratio and textural properties of the prepared supports and Co-catalysts.[a].

Sample	Si/Ti[b]	Si/Ti[c]	$S_{B.E.T.}$ (m^2/g)	$D_{B.J.H.}$ (nm)	V_p (cm^3/g)
ST1	5.7	5.9	703	4.2	0.87
ST2	1.0	0.9	339	3.4	0.28
ST3	0.2	0.3	51	2.6	0.04
SiO_2	–	–	673	3.9	0.77
TiO_2	–	–	82	11.7	0.08
STCo-Op1	5.7	5.5	533	4.9	0.69
STCo-Op2	1.0	1.3	364	4.1	0.37
STCo-Op3	0.2	0.2	214	2.8	0.11
STCo-Im1	5.7	5.9	570	3.3	0.71
STCo-Im2	1.0	0.9	203	2.9	0.19
STCo-Im3	0.2	0.3	37	2.1	0.02
SCo-Op	–	–	587	3.3	0.71
SCo-Im	–	–	539	3.0	0.68
TCo-Op	–	–	56	7.1	0.13
TCo-Im	–	–	57	7.2	0.14

[a] The used nominal content in all the prepared Co-catalysts was 10 wt.%.
[b] Nominal Si/Ti molar ratio.
[c] Experimental Si/Ti molar ratio obtained by EDS-XRF.

2.2. Preparation of the Co-catalysts supported on SiO_2,TiO_2 or SiO_2-TiO_2 by conventional impregnation with a cobalt nitrate solution

The impregnated Co-catalysts were prepared by mixing in an agate mortar the respective amount of the support and 1 mL of an aqueous solution of cobalt (II) nitrate to obtain a nominal value of 10 wt.% of supported Co [22]. The mixture was grinded, transferred to a Petri dish and dried in an oven at 80 °C for 24 h. Finally, the obtained powder was calcined under static air at 550 °C for 5 h. The Co-catalysts prepared by impregnation were named as it is shown in Table 1, where “Im” refers to this applied methodology.

2.3. Preparation of the Co-catalysts supported on SiO_2, TiO_2 or SiO_2-TiO_2 by a sol-gel one-pot synthesis using cobalt oxalate as Co_3O_4 precursor

Firstly, cobalt oxalate dihydrate, the cobalt oxide precursor salt, was synthesized by dissolving 1.26 g of oxalic acid in a solution containing 100 mL of distilled water and 1 mL of NH_4OH (25% solution). Then, a solution containing 2.34 g of $Co(NO_3)_2.6H_2O$ dissolved in 100 mL of distilled water was added under stirring. The formed pink precipitate was separated by filtration and washed several times with distilled water, followed by drying at 80 °C during 24 h.

The one-pot prepared Co-catalysts were synthesized following the same procedure used in the sol-gel synthesis of the pure supports described above, but mixing the amount of cobalt oxalate to obtain a nominal value of 10 wt.% of supported Co after the addition of the TTIP and ACAC. The obtained gel was separated by filtration and then washed with distilled water, followed by drying at 80 °C and calcination under static air at 550 °C for 5 h. The one-pot prepared Co-catalysts were named as it is shown in Table 1, where “Op” refers to this applied methodology.

For comparison purposes, a bulk cobalt titanate sample was prepared as described by Lin et al., [29] using a Co^{2+}:Ti^{4+}:citric acid molar ratio of 1:1:4. In a typical procedure, a solution containing 4.4 g

of citric acid dissolved in 20 mL of ethanol was mixed with a solution containing 3.0 mL of TTIP in 20 mL of ethanol. Thereon, a solution containing 2.5 g of cobalt (II) acetate in 20 mL of ethanol was added. The obtained final suspension was transferred to a Petri dish and the solvent evaporated in an oven at 70 °C. The obtained pink powder was calcined at 700 °C for 9 h (heating rate of 5 °C min^{-1}).

2.4. Catalytic evaluation in the CO oxidation

The evaluation of the catalytic activity was performed in a fixed bed quartz tubular reactor containing 50 mg of catalyst mixed with 100 mg of silicon carbide. The reactor was continuously fed with a gas flow (GHSV = 12,100 h^{-1}) that was constituted by 24 mL min^{-1} of 1% of CO (mol/mol) and 12 mL min^{-1} of 5% of O_2 (mol/mol) in He, *i.e.* the CO/O_2 ratio used in this study was 0.4. The reactor was put in a tubular furnace with a temperature controller and the reaction temperature varied between 100 and 550 °C with increments of 50 °C. The gaseous reactor effluent was analyzed on line in a Shimadzu gas chromatograph (GC-17 A) equipped with a thermal conductivity detector (TCD).

3. Results and discussion

3.1. Chemical analysis, crystalline structure and textural properties of the pure supports and Co-catalysts

As shown in Table 1, the experimental Si/Ti molar ratio of the ST1, ST2 and ST3 silica-titania supports was 5.9, 0.9 and 0.3, respectively, being these results in good agreement with the used nominal values (5.7, 1 and 0.2, respectively).

As depicted in the X-ray diffractograms of the silica-titania pure supports (Figure S1, Electronic supplementary information, ESI), the ones with nominal Si/Ti molar ratios of 5.7 and 1.0 (samples ST1 and ST2, respectively), showed only a halo centered at 2θ = 23.9° (indicated by an S in the Fig. S1), which is associated to the presence of amorphous silica. These XRD results suggest that the titania phase is highly dispersed over the amorphous silica structure. On the other hand, the increase of the titanium amount to a nominal Si/Ti molar ratio of 0.2 (support ST3) led to the formation of a solid constituted mainly by titania anatase (JCPDS 84-1286), as indicated by T in Figure S1 (Rietveld refinement resulted in 91.3 wt.% of anatase TiO_2 with χ^2 = 1.278 and wRp = 0.1089).

As can be seen in Fig. 1a, the diffractograms of all the silica-titania supported Co-catalysts one-pot prepared displayed diffraction peaks assigned to the presence of segregated anatase into the amorphous silica (JCPDS 84–1286, peaks indicated by T), and cobalt oxide (Co_3O_4, JCPDS 42–1467, peaks indicated by C). As expected, the Rietveld refinement data showed an increase in the titania anatase amount with the increase of the incorporated Ti in the Si-Ti supports (Table 2).

In spite of all the one-pot prepared catalysts having similar cobalt amounts, as determined by ICP-MS (Table 2), it is possible to observe a decrease in the intensity of the characteristic diffraction peaks of Co_3O_4 with the increase of the Ti amount in the support (Fig. 1a). On the other hand, that effect was not pronounced in the samples prepared by impregnation. These results may be explained on the basis that in the sol-gel one-pot methodology, since the support and the precursor of the active phase are mixed during the sol-gel synthesis of the support, a higher interaction occurs between the titanium and cobalt atoms. Such interaction might lead to the formation of cobalt titanate ($CoTiO_3$) during the calcination of the formed gel, thus lowering the number of cobalt ions available to form Co_3O_4, and consequently leading to a lower amount of Co_3O_4 crystallites.

The cobalt titanate formation on cobalt catalysts supported on titania was suggested by other groups [30–34] and its detection by XRD measurements is complex due to the low intensities of its diffraction peaks when compared to those of titania anatase [32]. In that way, despite the green color (Figure S2) of the one-pot prepared STCo-Op3 catalyst, which is characteristic of cobalt titanate, its diffraction peaks were not observed in the X-ray diffractogram. However, the presence of that compound in the samples was confirmed by using infrared and Raman spectroscopies, which will be further discussed.

Moreover, it is possible to notice a decrease in the crystallite size of Co_3O_4 with the increase of the titanium amount in the catalysts prepared by the one-pot method. In this context, the catalyst STCo-Op1

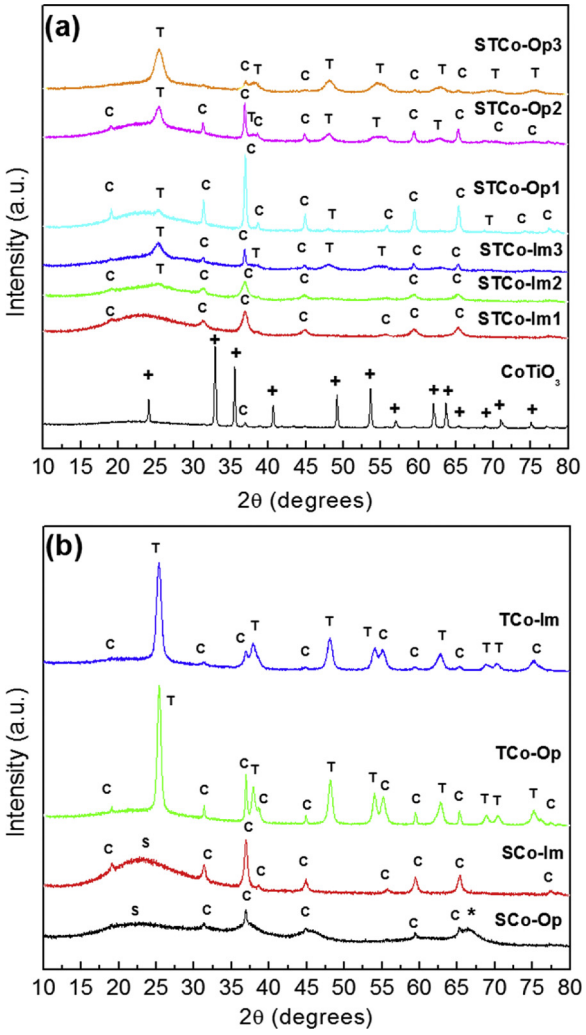

Fig. 1. XRD diffractograms of the Co-catalysts supported on: (a) silica-titania; (b) silica or titania (C = Co_3O_4, T = TiO_2 anatase and S = amorphous SiO_2).

Table 2
Cobalt content and the Co_3O_4 crystallite size in the prepared Co-catalysts.

Catalyst	Co (wt. %)[a]	Co_3O_4 crystal size (nm)[b]	Anatase (%)[b]	Rietveld refinement parameters	
				χ^2	wRp
STCo-Op1	10.8	33.2	7.9	1.097	0.099
STCo-Op2	9.8	23.7	49.3	1.141	0.181
STCo-Op3	10.3	4.9	87.8	1.376	0.198
STCo-Im1	9.3	12.2	0	1.202	0.096
STCo-Im2	9.2	11.5	3.6	1.189	0.123
STCo-Im3	9.8	17.8	84.6	1.349	0.201
SCo-Op	9.1	19.1	–	1.156	0.149
SCo-Im	9.9	20.1	–	1.075	0.102
TCo-Op	8.5	21.2	91.2	1.364	0.158
TCo-Im	8.6	15.5	89.1	1.029	0.089

[a] Determined by ICP-MS.
[b] Determined by Rietveld refinement.

presented the largest Co_3O_4 crystallite size (33.2 nm) and the catalyst STCo-Op3 presented the smallest crystallite size (4.9 nm), as shown in Table 2. Considering only the active phase crystallite size, it is expected that a better catalytic activity will be reached by the catalyst with the smallest crystallite size. However, two important features must be considered: (i) despite the smallest crystallite size of the catalyst STCo-Op3, it presented the lowest number of active sites because of the largest amount of formed cobalt titanate during its synthesis, which possess a very low activity in the CO oxidation reaction [34]) and (ii) as reported in the literature, a higher CO oxidation activity is not only a function of the Co_3O_4 crystallite size, but rather depends strongly on the amount of highly active Co^{3+} species exposed on the catalyst surface [35].

The diffractogram of the one-pot prepared Co-catalyst supported on pure SiO_2 (SiCo-Op) (Fig. 1b) is mainly constituted by the characteristic halo of the amorphous silica and diffraction peaks related to Co_3O_4. In addition, a broad peak at $2\theta = 66.5^{\circ}$ attributed to the diffraction of cobalt silicate, $CoSiO_3$ (JCPDS 72–1508), was also verified in the diffractogram of this sample, which is coherent with the blue color displayed by this material (Fig. S2) [36,37]. The $CoSiO_3$ formation was suggested to occur through the reaction between silicic acid $[SiO_x(OH)_{4-2x}]_n$ and cobalt precursors during the gel calcination [36,37]. On the other hand, only diffraction peaks assigned to the presence of Co_3O_4 were observed in the diffractogram of the Co-catalyst supported on SiO_2 prepared by impregnation, and no $CoSiO_3$ diffraction peaks were evidenced.

The diffractograms of the Co-catalysts supported on pure titania prepared either by one-pot or impregnation (Fig. 1b) are constituted by diffraction peaks related to the presence of Co_3O_4 and titania anatase. Furthermore, no diffraction peaks related to cobalt titanate were observed in the diffractograms of these samples, suggesting its small formation during the catalysts preparation [32,38].

Next, the textural properties of the pure supports and Co-catalysts were evaluated. As can be seen in Figure S3, the silica-titania supports with nominal Si/Ti molar ratios of 5.7 and 1.0 (ST1 and ST2, respectively) and the pure silica that were employed to prepare the impregnated Co-catalysts presented type IV isotherms according to the IUPAC classification [39], with a H2 type hysteresis loop, characteristic of solids with well-defined porous distribution and shape [39]. The nitrogen adsorption/desorption isotherms of the ST3 support could be assigned as pseudo type I (Figure S3c) due to its similarity with that of microporous materials, as was also observed by Klein et al. [40] and Lafond et al. [41], in which the increase of the titanium amount in the silica support led to a marked decrease in the specific surface area (Table 1) as a consequence of the poor textural properties of the anatase [26]. On the other hand, the isotherms of pure titania (Fig. S3) were classified as type IV, which are characteristic of mesoporous materials with H3 type hysteresis loop, typical of slit-shaped pores.

The textural properties of the pure silica, pure titania or silica-titania supports and of the one-pot supported cobalt catalysts (Table 1) showed that the materials containing a lower amount of titanium presented higher values of specific surface area. As already mentioned, the observed decrease in the values of specific surface area presented by the Co-catalysts prepared *via* the one-pot approach supported on titania or silica-titania with high titanium amount is related to the intrinsic poor textural properties of the titania anatase [26,42,43].

As already expected, a marked decrease was observed in the specific surface area, pore diameter and pore volume for the catalysts prepared by impregnation when compared to the pure supports (Table 1), which is attributed to the partial blockage of the support pore entrances by the Co_3O_4 nanoparticles or their agglomerates. [32,43–45]

3.2. Spectroscopic characterization

The infrared spectra of the silica, titania and silica-titania pure supports are shown in Figure S4. It possible to observe some common bands in the respective spectra, *i.e.* the stretching of Si−OH (3455 cm^{-1}), Ti−OH (3430 cm^{-1}) and −OH (3600 cm^{-1}) groups, Si-O-Si (1050 cm^{-1}) and Ti-O-Ti (475 cm^{-1}). [46–48] Furthermore, the band marked by an asterisk in the spectra of the silica-titania supports is usually assigned to the stretching of Si-O-Ti bonds and therefore, is used as an indicative that the titanium atoms are well dispersed and incorporated into the amorphous silica structure [46–48].

The infrared spectra of the prepared bulk cobalt titanate and of the Co-catalysts are shown in Figure S5. The spectrum of $CoTiO_3$ (Fig. S5a) shows bands at 518 and 437 cm^{-1} that are assigned to the Ti-O stretching in TiO_6 groups, and a band at 694 cm^{-1} that is ascribed to the Co-O-Ti stretching. [46–49] As can be observed, the band at 437 cm^{-1}, which is assigned to the Ti-O stretching in the $CoTiO_3$ structure (highlighted by the grey stripe in the Figure S5a), is also present in the spectra of all of the Co-catalysts supported on silica-titania. Furthermore, the bands at 675 cm^{-1} and 587 cm^{-1} in the spectra of all of the Co-catalysts are characteristic of Co_3O_4, which are assigned, respectively, to the Co-O stretching of Co^{3+} in octahedral sites and Co^{2+} in tetrahedral sites, [50,51] and the broad band at 573 cm^{-1} in the spectrum of the SCo-Op catalyst (Fig. S5b) is characteristic of the stretching of the Si-O-Co bond in the cobalt-silicate structure [36,37]. Additionally, the bands marked by an asterisk in the spectra of the Co-catalysts supported on pure titania (Fig. S5b) are assigned to the Co-O-Ti stretching in cobalt titanate [52].

The Raman spectrum of the ST1 support (Fig. S6) shows a broad band centered at 153 cm^{-1} that is related to titania, and this band appears more well-defined in the spectrum of the ST2 support as a result of the higher titanium amount in the amorphous silica support [53]. As expected, the spectrum of the ST3 support is similar to the one of pure titania, a consequence of the high titanium amount present as anatase, corroborating the XRD results (Fig. 1) and the Rietveld refinement that were shown in the discussion of the XRD data. The five bands present in the spectra of the supports ST3 and pure TiO_2 are characteristic of the anatase phase. As for the Co-catalysts (Fig. 2a) whose support has a lower Ti amount, besides the well-defined titania and Co_3O_4 bands, the Raman spectra also showed an intense band between 685 and 695 cm^{-1} that is characteristic of the A_g mode of cobalt titanate [54,55]. In the STCo-Op3 and STCo-Im3 catalysts, that band is overlapped with the band related to the E_g mode of titania anatase [32]. The Raman spectrum of $CoTiO_3$ has ten active Raman modes, being five of them assigned to the vibrational mode A_g and the other five assigned to the vibrational mode E_g [54,55].

The bands at 192, 480 and 521 cm^{-1} in the Raman spectra of the cobalt catalysts supported on pure silica (Fig. 2b) are assigned, respectively, to the F_{2g}, E_g and F_{2g} vibration modes of Co_3O_4 [56]. In addition, Pedroza et al. [57] assigned the band between 685 and 690 cm^{-1} to the vibrational mode of the Si-O-Co bond in the cobalt silicate structure, as can be observed in the spectra of the SCo-Op and SCo-Im catalysts (Fig. 2b). The Raman spectra of the Co-catalysts supported on pure titania (Fig. 2b) are considerably similar to the spectrum of the support constituted by pure titania anatase (Figure S6), being comprised mostly by bands assigned to vibrational modes of that phase. The broad band in the range of 600 to 700 cm^{-1} in the spectra of the lastest discussed catalysts is resultant from the overlapping between bands of titania anatase and cobalt titanate [32,38].

Next, some selected representative cobalt catalysts supported on silica-titania prepared by the one-pot or impregnation approaches were analyzed using XPS on the $Co2p_{3/2}$ core level, aiming to obtain more insights concerning the oxidation state of the supported cobalt species. The XPS spectra of the one-pot prepared STCo-Op1 and STCo-Op3 catalysts are shown in Fig. 3a and b, respectively, and the ones prepared by impregnation (STCo-Im1 and STCo-Im3) are shown in Fig. 3c and 3d, respectively.

The deconvolution of the obtained XPS spectra (Fig. 3) resulted in three distinct peaks that could be assigned to Co^{3+} (779.19–779.81 eV) and Co^{2+} (781.13–781.49 eV) in a $2p_{3/2}$ configuration, and the peak

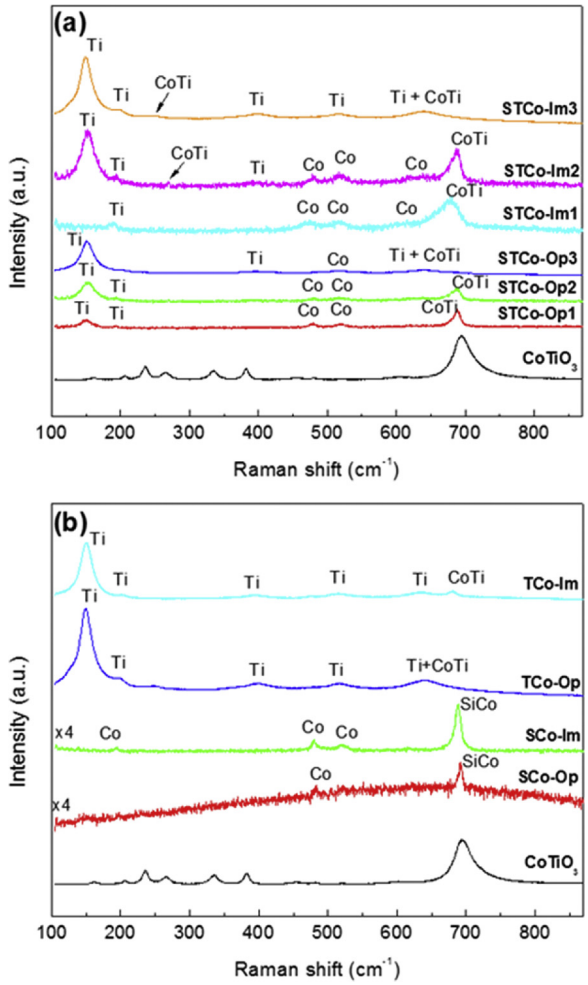

Fig. 2. Raman spectra of the prepared Co-catalysts supported on: (a) silica-titania; (b) silica or titania, in which the bands marked by Co denote bands of Co_3O_4, by Ti bands of TiO_2 anatase, by CoTi bands of $CoTiO_3$ and by SiCo bands of $CoSiO_3$.

located at the binding energies in the range of 783–784.18 eV are assigned to the Co^{2+} shake-up satellite peak of Co_3O_4 [58–62]. Table 3 shows Co $2p_{3/2}$ spectral fitting parameters such as peak position, FWHM, area and Co^{2+}/Co^{3+} ratio, in which the latter was calculated using the areas resulting from the peaks assigned to the Co^{2+} and Co^{3+} components and neglecting the shake-up peaks [61,62].

In this context, the Co^{2+}/Co^{3+} ratio gives essential information concerning the different cobalt species formed as a function of the titanium amount in the silica support. From Table 3, it is possible to observe a lower Co^{2+}/Co^{3+} ratio for the Co-catalysts supported on silica-titania with low amount of titanium (samples STCo-Op1 and STCo-Im1, with nominal Si/Ti equal to 5.7) compared to those supported on silica-titania containing high amounts of titanium (samples STCo-Op3 and STCo-Im3 with nominal Si/Ti equal to 0.2). Furthermore, since only Co^{2+} cations are present in the cobalt titanate structure, the higher Co^{2+}/Co^{3+} ratios observed on the catalysts supported on silica-titania with high titanium amount are an important indicative of the cobalt titanate formation, as also evidenced by infrared and Raman spectroscopies.

Figure S7 shows the O1s XPS spectra of the same Co-catalysts showed in Fig. 3. In those spectra, the deconvoluted curves with maximum binding energies between 529.40–529.98 eV, 531.30–531.70 eV, 532.25–532.70 eV and 533.00–533.80 eV are assigned to O^{2-} lattice ions, low-coordinated or adsorbed O- ions, hydroxyl groups and adsorbed water, respectively [35].

A difference in the O1s spectra of the Figure S7 can be observed as a function of the titanium amount into the amorphous silica. As can be observed, a higher fraction of lattice oxygen is observed in the spectra of the cobalt catalysts supported on silica-titania with lower titanium amount (samples STCo-Op1 and STCo-Im1). On the other hand, a higher fraction of hydroxyl groups is observed in the spectra of the cobalt catalysts supported on silica-titania with higher titanium amount (samples STCo-Op3 and STCo-Im3). As will be discussed in the analysis of the behavior of the Co-catalysts, the concentration of superficial Co^{3+} and lattice O^{2-} will interfere directly in their specific activity.

3.3. SEM-EDS and TEM-EDS characterization

SEM-EDS and TEM-EDS analyses were performed in order to comprehend the dispersion of the cobalt oxide active phase on the silica-titania supports. In the SEM-EDS chemical mapping (Fig. 4) it is possible to observe a more superficial exposure of cobalt atoms over the silica-titania support on the catalysts prepared by the one-pot procedure (catalysts STCo-Op1 and STCo-Op3), which are comprised by agglomerates of the active phase Co_3O_4. On the other hand, a less evident exposure of cobalt atoms was observed for the catalysts prepared *via* impregnation (catalysts STCo-Im1 and STCo-Im3) [32,43–45].

In addition, it was observed for the STCo-Im1 catalyst (Fig. 4c) that the titanium atoms are well dispersed into the analyzed layer of the silica-titania support, with no evident formation of agglomerates. On the other hand, the presence of a Ti domain could be observed in the catalyst STCo-Op1 (Fig. 4a), corroborating the XRD analysis, in which the occurrence of a titania-anatase segregation into the amorphous silica was suggested. Furthermore, a poor dispersion of titanium atoms and the formation of larger Ti-agglomerates were observed for the STCo-Op3 and STCo-Im3 catalysts (Fig. 4b and d), the ones with higher Ti amount in the support, suggesting the formation of large agglomerates of titania-anatase crystallites, also in accordance with the XRD results (Fig. 1).

Fig. 5 shows illustrative TEM images of the STCo-Op1 and STCo-Op3 Co-catalysts prepared by one-pot and of the STCo-Im1 and STCo-Im3 prepared by impregnation. In Fig. 5, the red squares are the limiting area in which the EDS analyses were performed. As can be observed in the TEM image of the STCo-Op1 catalyst (Fig. 5a), the cobalt species are superficially dispersed on the silica-titania support and the particles have quasi-spherical shape (indicated by the arrows in the TEM image). The EDS analysis from square 1 (Fig. 5a) shows the presence of Si and Ti atoms from the silica-titania support and the presence of Co atoms was not detected. In addition, the square 2 in Fig. 5a contains a high count of Co atoms, as shown in its EDS spectrum. On the other hand, considering the STCo-Op3 catalyst, and according with the non-observable presence of Co_3O_4 particles, the EDS spectra of the areas related to the squares 1 and 2 (Fig. 5b) only show the presence of Si and Ti atoms.

It is possible to observe in the TEM image of the STCo-Im1 catalyst prepared by impregnation (Fig. 5c) the presence of large agglomerates of Co_3O_4 (indicated by the arrows) covered by Si and Ti atoms from the silica-titania support with concealed aspect. That observation could be supportive that Co_3O_4 nanoparticles are blocking the pores of the support and in agreement with the lower surface area, pore volume and pore diameter of the considered sample showed in the Table 1. The EDS spectrum of the area delimited by the square 1 in Fig. 5c (sample STCo-Im1), only shows the presence of Si and Ti atoms from the support, nevertheless, a simultaneous presence of Co, Si and Ti atoms in that catalyst was confirmed by the EDS spectrum of the area delimited by the square 2. Furthermore, the TEM image of the catalyst STCo-Im3 (Fig. 5d) also displayed the same trend observed in the TEM image of the catalyst STCo-Im1, in which the large agglomerates of Co_3O_4 are covered by Si and Ti atoms from the silica-titania support, with the presence of Co, Si and Ti atoms being confirmed by the EDS spectrum of the analyzed area of the square 2 of said figure.

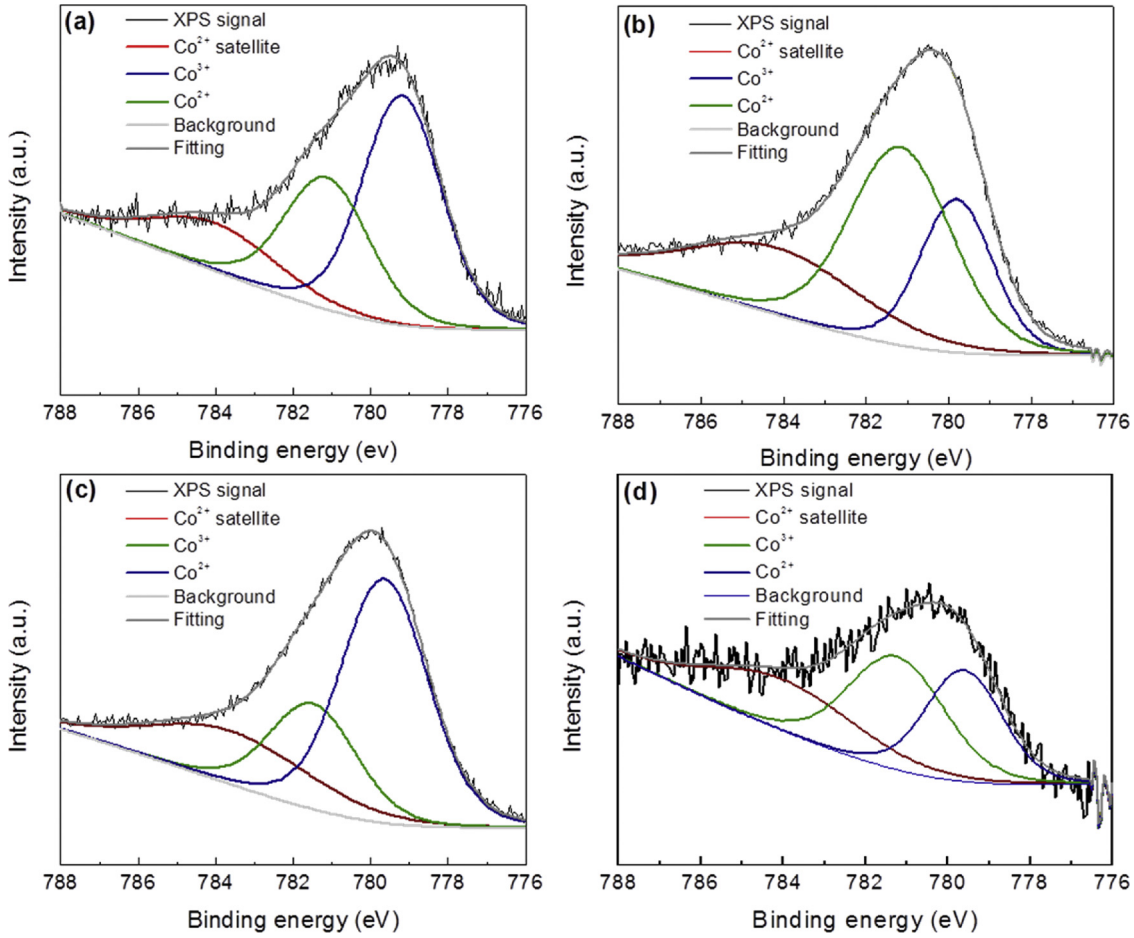

Fig. 3. XPS spectra of the Co2p$_{3/2}$ core level of the Co-catalysts supported on silica-titania: (a) STCo-Op1; (b) STCo-Op3; (c) STCo-Im1; (d) STCo-Im3.

Table 3
Co 2p$_{3/2}$ spectral fitting parameters: peak position, FWHM, area and Co^{2+}/Co^{3+} for the Co-catalysts supported on silica-titania prepared by one-pot or impregnation.

		STCo-Op1	STCo-Op3	STCo-Im1	STCo-Im3
Peak 1 (Co^{2+} satt.)	Position (eV)	784.0 ± 0.5	784.2 ± 0.5	783.9 ± 0.5	784.0 ± 0.5
	FWHM (eV)	3.87 ± 0.5	4.98 ± 0.5	4.97 ± 0.5	4.39 ± 0.5
	Area	3735.8	14218.5	19104.6	1438.6
Peak 2 (Co^{2+})	Position (eV)	781.1 ± 0.5	781.2 ± 0.5	781.5 ± 0.5	781.2 ± 0.5
	FWHM (eV)	2.61 ± 0.5	2.93 ± 0.5	2.66 ± 0.5	2.78 ± 0.5
	Area	6982.6	24714.3	20311.5	2002.6
Peak 3 (Co^{3+})	Position (eV)	779.2 ± 0.5	779.8 ± 0.5	779.7 ± 0.5	779.6 ± 0.5
	FWHM (eV)	2.42 ± 0.5	2.09 ± 0.5	2.67 ± 0.5	2.21 ± 0.5
	Area	11256.4	13693.1	47027.5	1560.5
Ratio Co^{2+}/Co^{3+} [A,B]		0.62 ± 0.06	1.80 ± 0.06	0.43 ± 0.06	1.28 ± 0.06

The TEM images of the Co-catalysts prepared by the one-pot methodology and by impregnation clearly indicated that the last method led to Co-catalysts comprised by large agglomerates of Co_3O_4 nanoparticles covered by a layer of silica-titania support, and consequently with a lower amount of exposed cobalt active sites.

3.4. H_2-TPR measurements

The reduction profile of the bulk Co_3O_4 shows two distinct events, which correspond to the two reduction steps described in the Eqs. (1) and (2) [63]. The first one is attributed to the reduction of Co^{3+} to Co^{2+} and the second one to the reduction of Co^{2+} to Co°.

$$Co_3O_4 + H_2 \rightarrow 3CoO + H_2O \quad (1)$$

$$3CoO + 3H_2 \rightarrow 3Co + 3H_2O \quad (2)$$

Fig. 6 shows the H_2 reduction profiles of the prepared Co-catalysts, and Table 4 the reducibility of the Co species in the analyzed samples (R %).The reduction profile of the bulk cobalt titanate (Figure S8) is formed by two reduction peaks at 328 °C and 648 °C. The first one is assigned to the reduction of Co_3O_4 present as impurity, corroborating the XRD results (Fig. 1a), and the second peak is ascribed to the reduction of the Co^{2+} species present in cobalt titanate as indicated by Eq. (3). [64]

$$CoTiO_{3(s)} + H_{2(g)} \rightarrow Co^{\circ}_{(s)} + TiO_{2(s)} + H_2O_{(g)} \quad (3)$$

As can be noticed from Fig. 6a, a pronounced displacement of the Co reduction peaks to higher temperatures occurred for the Co-catalysts prepared by impregnation, being assigned, as already discussed, to the formation of cobalt species covered by the silica-titania support, as was evidenced from the TEM-EDS data, with the hydrogen molecules being

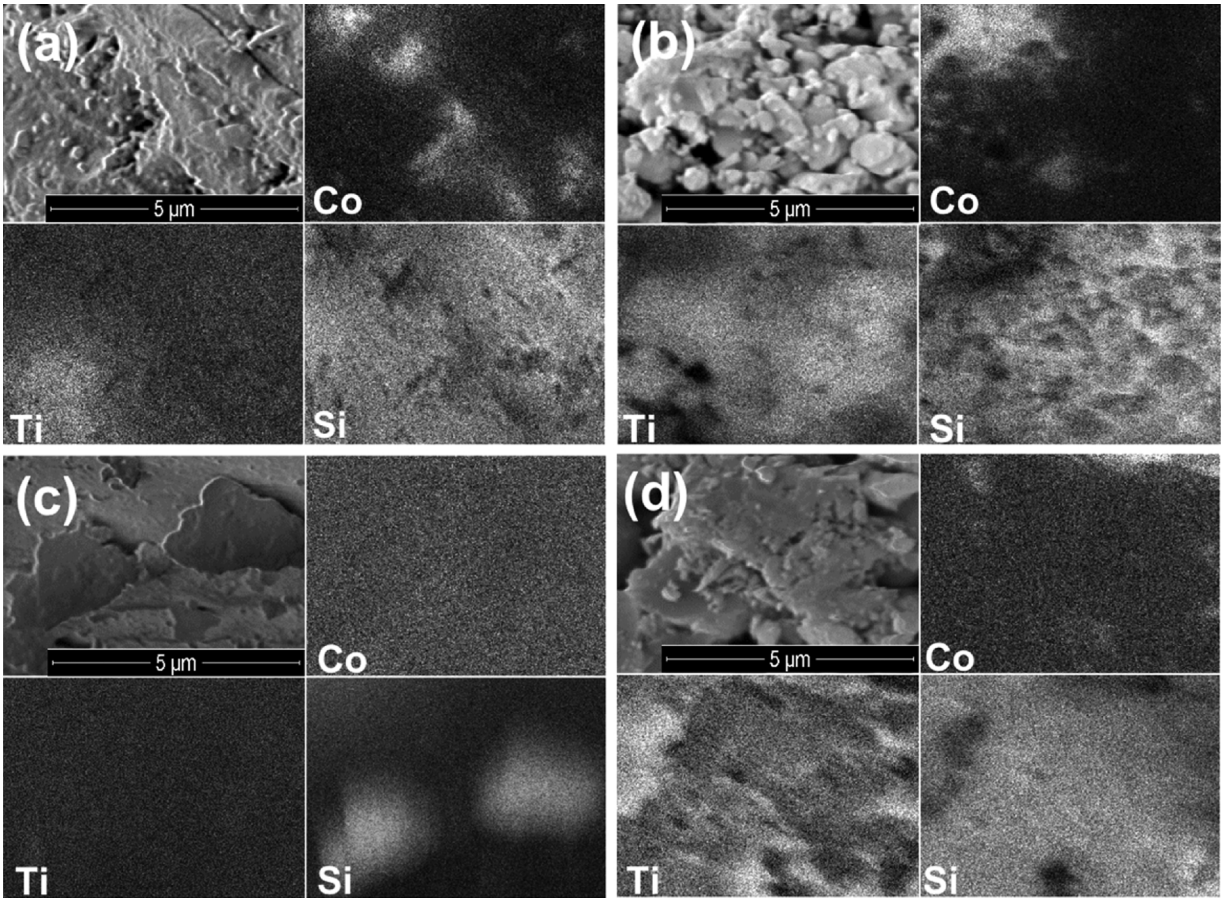

Fig. 4. SEM-EDS chemical mapping of the prepared Co-catalysts: (a) STCo-Op1; (b) STCo-Op3; (c) STCo-Im1; (d) STCo-Im3. In the images, the atom count is directly related to the intensity of the white color.

hindered from reaching the cobalt species. On the other hand, the H_2-TPR profiles of the Co-catalysts prepared by the one-pot route showed simpler reduction profiles and a marked decrease in the Co-reducibility with the increase of the titanium amount in the silica-titania support was observed (Table 4).

The observed decrease in the Co reducibility is attributed to the formation of cobalt species with strong interaction with the titanium-containing support, such as $CoTiO_3$ [30–34], whose reduction can be

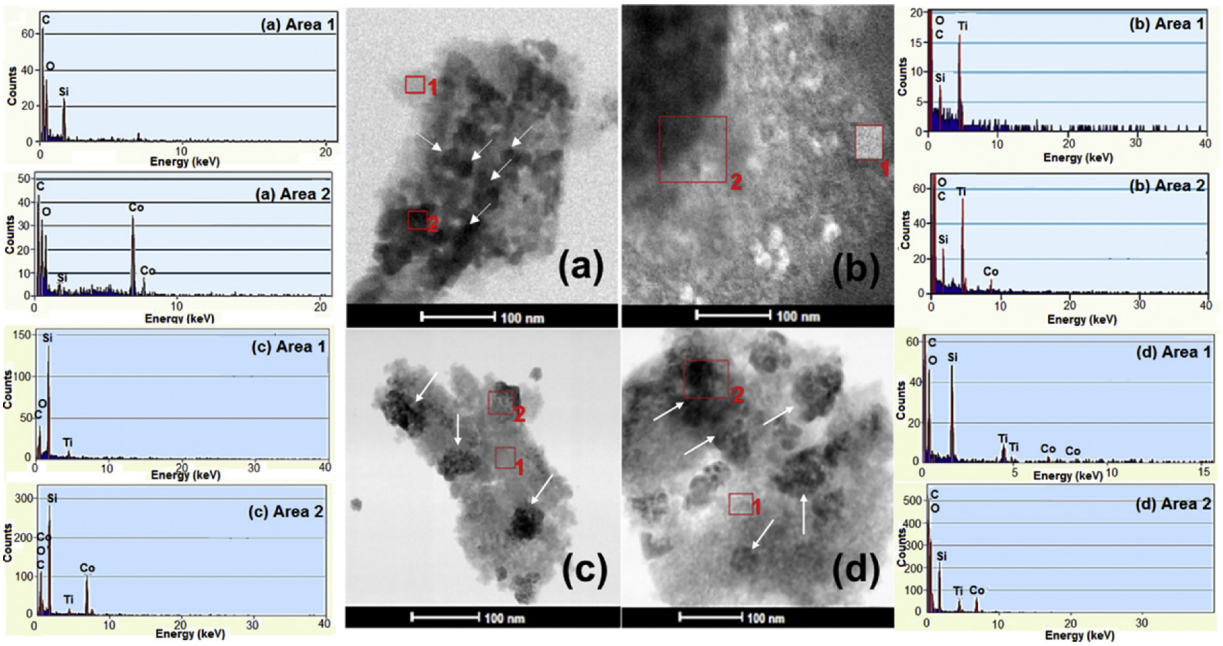

Fig. 5. TEM images and EDS analyses of the prepared Co-catalysts: (a) STCo-Op1; (b) STCo-Op3; (c) STCo-Im1; (d) STCo-Im3.

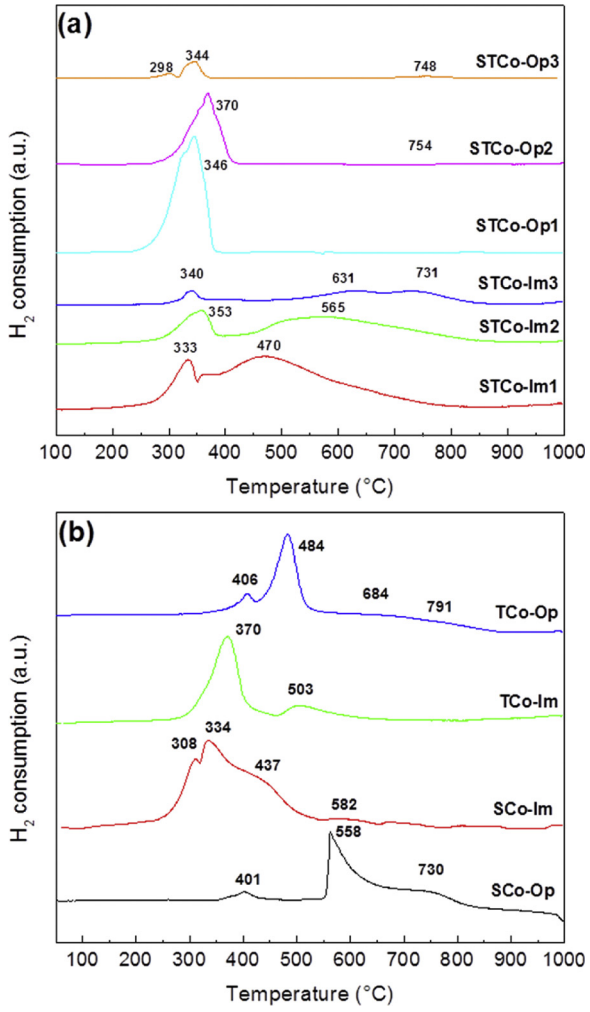

Fig. 6. H_2-TPR profiles of the prepared Co-catalysts supported on: (a) silica-titania; (b) silica or titania.

Table 4
Co-Reducibility (R), CO conversion at 550 °C, light-off temperature (T_{50}) and specific activity (S.A.) to CO oxidation at T_{50} on the studied Co-catalysts.

Catalyst	R (%)	CO conv. at 550 °C (%) [a]	T_{50} (°C)	S.A. at T_{50} ($mol_{CO}.mol_{cobalt}^{-1}.s^{-1}$)x$10^{-4}$
STCo-Op1	91.7	100	209	1.85
STCo-Op2	61.0	100	279	1.37
STCo-Op3	19.5	100	315	1.30
STCo-Im1	77.1	100	306	1.45
STCo-Im2	55.4	100	327	1.44
STCo-Im3	34.6	91.7	[b]	[b]
SCo-Op	55.4	89.8	[b]	[b]
SCo-Im	72.9	100	272	1.40
TCo-Op	49.2	94.3	[b]	[b]
TCo-Im	61.2	60.8	[b]	[b]
$CoTiO_3$	—	93.6	[b]	[b]

[a] Values obtained from Figure S8.
[b] Catalysts which did not reach 100% of CO conversion at 550 °C.

observed at temperatures above 700 °C in the H_2-TPR reduction profiles. That reduction peak was mainly observed in the reduction profiles showed in Fig. 6 for the one-pot prepared Co-catalysts on supports with high titanium amount (samples STCo-Op3 and TCo-Op).

In that way, the catalyst STCo-Op1 with the lowest Ti amount and prepared by the one-pot methodology had the highest Co-reducibility among the studied Co-catalysts. This result is in agreement with other reports, which have showed that silicon-containing supports loaded with tunable low amounts of titanium promote an increase in the dispersion of the respective studied active species. [16,28,65,66]

The Co-catalysts supported on pure SiO_2 or TiO_2 (Fig. 6b) showed considerably different reduction profiles from the catalysts supported on silica-titania. The Co-catalyst supported on silica prepared by one-pot (sample SCo-Op) shows reduction peaks at higher temperatures than the similar catalyst obtained by the impregnation route (sample SCo-Im). This observation is related to the simultaneous formation of Co_3O_4 and cobalt species in strong interaction with the silica support, such as $CoSiO_3$, that are formed during the calcination step involving solid-state reactions in the SCo-Op catalyst. [67] As expected, the formation of cobalt titanate also caused a decrease in the Co-reducibility of the Co-catalyst supported on pure TiO_2 prepared by the one-pot route.

3.5. Catalytic performance in the CO oxidation

Having the physical and chemical characterization of the Co-catalysts supported on silica, titania or silica-titania in hands, their catalytic activity was then evaluated in the oxidation of carbon monoxide with oxygen.

As mentioned in the experimental procedure, the CO/O_2 used in this study was 0.4, since a higher CO/O_2 may cause a decrease in the catalytic activity as consequence of a competitive mechanism for the active sites between the CO and O_2 molecules. [17,68–71] A higher CO concentration in the fed gaseous mixture could hinder the adsorption of active O_2 molecules and their dissociation, and in this sense, the catalyst surface would be in a reduced state by the adsorption of CO molecules on the Co^{3+} active sites. Since a Mars Van Krevelen mechanism plays a pivotal role in the CO oxidation over Co_3O_4 catalysts, the CO molecules firstly adsorb on the Co^{3+} active sites and these adsorbed molecules react with a lattice oxygen from Co_3O_4 surface, thus forming adsorbed CO_2. In this context, the use of a low CO concentration leads to a higher catalytic activity in the CO oxidation, since a higher O_2 concentration in the reaction mixture is able to promote the restoration of the oxidation state in the catalyst surface. Furthermore, considering the strength of the bond formed between gaseous molecule and catalyst surface, it is noteworthy to mention that the O_2 adsorption is much less stronger than CO adsorption and will not lead to a blockage of the active sites when a low CO/O_2 ratio is used. [17,35,70–72]

The specific activity (SA) of the samples in the CO oxidation to CO_2 as a function of the reaction temperature is shown in Fig. 7. The specific activity (SA) in the used heterogeneous reactor working at steady-state conditions was closely estimated by Eq. (4), representing the number of CO mols converted to CO_2 per second divided by the mols of Co supported on the evaluated catalyst ($mol_{CO}.mol_{cobalt}^{-1}.s^{-1}$).

$$SA = X.F / m \quad (4)$$

In this equation, X is the conversion of CO to CO_2 (Figure S8), F is the molar flow of CO fed to the reactor ($mol_{CO}.s^{-1}$) and m is the Co mol number (mol_{cobalt}) on the used catalyst (determined by ICP-MS). In this work, a reference light-off temperature (T_{50}) is defined for the used catalytic system and operation conditions, which represents the temperature in which the studied catalyst achieved 50% of its specific activity corresponding to 100% of conversion at 550 °C. In this context, the smaller the light-off temperature, the more efficient the catalyst was considered (Table 4). The values of T_{50} calculated from the conversion curves presented in the Figure S8 and specific activities calculated at the same temperature (200 °C) are presented in the Table S1.

As can be seen from Fig. 7a and Table 4, the one-pot prepared STCo-Op1 catalyst displayed a considerably higher CO oxidation specific activity at lower temperatures than any of the other studied Co-catalysts; the material showed the most increasing rate to CO oxidation from 100 °C and reached 50% of its total specific activity for 100% of conversion of CO to CO_2 at 209 °C (T_{50}). The high CO oxidation activity

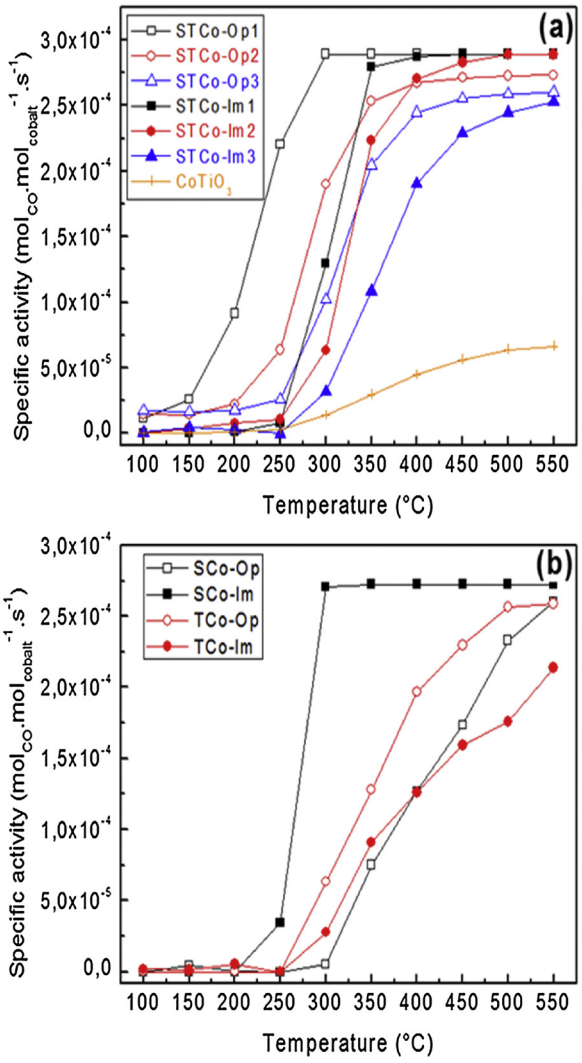

Fig. 7. Specific activity of the prepared Co-catalysts supported on: (a) silica-titania; (b) silica or titania, as function of the temperature.

of the STCo-Op1 catalyst is related to its highest Co reducibility when compared to the other Co-catalysts (Table 4), a consequence of its relatively lower Co reduction temperatures (Fig. 6) and its better textural properties (Table 1). As already discussed in the XRD analyses, N_2 sorption, SEM-EDS, TEM-EDS, and Raman spectroscopy, these properties in the STCo-Op1 catalyst resulted from the small amount of titanium incorporated into the silica support (nominal Si/Ti = 5.7) that did not generate cobalt titanate.

On the contrary, the higher titanium amount incorporated into the silica support of the one-pot prepared STCo-Op2 catalyst (Table 2) diminished its specific activity and reached its T_{50} at 279 °C (Table 4). This loss of activity with the increasing amount of Ti incorporated into the silica support was more evident in the STCo-Op3, which had the highest amount of incorporated Ti, leading to a T_{50} of 315 °C (Table 4). On the other hand, as it is observed from Fig. 7a and Table 4, the impregnated STCo-Im1 and STCo-Im2 catalysts presented very similar specific activity, showing T_{50} values of 306 °C and 327 °C, respectively, that are considerable higher than the T_{50} of the STCo-Op1 catalyst. In addition, the STCo-Im3 catalyst with the highest amount of incorporated Ti into the silica among the impregnated Co-catalysts did not reach 100% of CO conversion at 550 °C (Figure S8). The inferior catalytic behavior of the impregnated Co-catalysts is attributed to the formation of large Co_3O_4 agglomerates, as was verified from their chemical mapping in the SEM images (Fig. 4), TEM images and EDS spectra in the selected analyzed regions (Fig. 5), as well as by their Co-reduction peaks at higher temperatures (Fig. 6).

Considering the higher activity of the catalyst STCo-Op1 when compared to the other studied catalysts, a further catalytic evaluation was performed aiming to analyze the long-term stability of this catalyst in the CO oxidation. For this, the catalytic evaluation was performed at 550 °C for 12 h in the same conditions described in the experimental procedure. In this context, even after 12 h, the CO oxidation specific activity remained the same, evidencing the high stability of this catalyst at high temperature and a promising tolerance to deactivation, that could be a consequence of CO_2 adsorption or superficial carbonate formation. [18]

Similarly to the behavior reported by Yang et al., [34] the bulk cobalt titanate prepared in this work showed CO oxidation activity only at temperatures higher than 250 °C (Fig. 7a). From Fig. 7b, it is noteworthy to mention that the second most active catalyst was the SCo-Im catalyst, in which the high catalytic activity is assigned mainly to the high specific surface area of this material (Table 1), which allowed a better dispersion of the active phase Co_3O_4, thus leading to a high reducibility (72.9%) at low temperatures (< 450 °C) and to a low light-off temperature (272 °C). In contrast, the one-pot Co-catalyst supported on pure silica had lower specific activity to CO oxidation, a consequence of the cobalt silicate formation, which was evidenced by XRD (Fig. 1b), and suggested by its H_2-TPR profile (Fig. 6b). In addition, the Co-catalysts supported on pure titania also presented low specific activity values due to the formation of cobalt species with strong interaction with the titania support.

As discussed from the XPS data (Fig. 3), a lower Co^{2+}/Co^{3+} ratio was verified for the cobalt catalysts supported on silica-titania with low amount of titanium in the silica support (catalysts STCo-Op1 and STCo-Im1), which indicates a higher concentration of Co^{3+} on the catalyst surface. As aforementioned, the high activity of Co_3O_4 catalysts in the CO oxidation reaction is a consequence of the existence of the redox pair $Co^{2+} \leftrightarrow Co^{3+}$ in which the cobalt species readily change their oxidation state in the reaction mechanism. Furthermore, the highest active Co_3O_4 catalysts are those in which a higher amount of Co^{3+} are superficially exposed since these species are far more active for the CO adsorption than the Co^{2+} species. In this context, several studies have been reported emphasizing the superior catalytic activity of Co_3O_4 with higher exposure of Co^{3+} cations. [19,73–75] These studies involved carbon monoxide adsorption analyses on Co_3O_4 nanorods, [19] nanobelts and nanocubes [73] and nanoparticles [35] with crystalline planes exposing a Co^{3+}-rich surface. [76] All of these studies suggest that CO molecules preferably chemisorb on Co^{3+} sites, and on the other hand, the Co^{2+} sites are much less active to the adsorption of CO. In good agreement with those studies, the catalyst STCo-Op1 with the lowest Co^{2+}/Co^{3+} ratio and, consequently, the highest amount of Co^{3+} superficially exposed, presented the highest catalytic activity to CO oxidation. Other interesting feature evidenced from the XPS data of the analyzed Co-catalysts supported on silica-titania was the obtained spectra of the O1s core level. [35] A higher fraction of lattice oxygen was evident from the spectra of the Co-catalysts supported on silica-titania with the lowest titanium amount (STCo-Op1 and STCo-Im1) when compared to those with high amount of titanium (STCo-Op3 and STCo-Im3). A greater amount of lattice oxygen is also a desirable feature in a Co_3O_4 catalyst for CO oxidation, since these species are more active in the reaction mechanism (acting as oxygen source for the CO oxidation) when compared to other oxygen species such as surface hydroxyls or adsorbed O^- ions. [35] These findings show that the used one-pot methodology led to potential better CO oxidation Co-catalysts when compared to those prepared by impregnation. Furthermore, the incorporation of a controlled low amount of titanium atoms into the amorphous silica (sample prepared using a nominal Si/Ti molar ratio of 5.7) through the one-pot methodology significantly enhanced the specific activity to CO oxidation and more importantly, substantially decreased the light-off temperature. Such pronounced performance was

attributed to the higher Co dispersion and the absence of Co-species with strong interaction with the silica-titania support, leading to higher Co reducibility with H_2 (Table 4) and to a lower Co^{2+}/Co^{3+} ratio and higher amount of lattice O^{2-}. On the other hand, the incorporation of a higher amount of Ti (samples prepared using a nominal Si/Ti molar ratio of 0.2) led to the formation of cobalt species with strong interaction with the silica-titania support as cobalt titanate, consequently having higher Co reduction temperatures, higher Co^{2+}/Co^{3+} ratio and lower amount of lattice O^{2-}, then presenting lower activity to CO oxidation.

In addition, in this study it was found that the crystallite size of Co_3O_4 was not the crucial feature for a good catalytic performance to CO oxidation. The highest catalytic activity showed by the catalyst STCo-Op1 appears to be an oxymoron, since this catalyst had larger Co_3O_4 crystallite size when compared to the one of the STCo-Op3 catalyst, also prepared by the one-pot route. As reported by Iablokov and co-workers [77] in their studies of size-reactivity correlation of Co_3O_4 nanoparticles in the CO oxidation reaction, the size of the cobalt oxide nanoparticles possess a secondary effect in the catalytic activity and the most important feature for a high catalytic activity is the exposure of Co^{3+} cations in the Co_3O_4 surface. That finding is in accordance with the results obtained in this study, in which despite its largest crystallite size, the catalyst STCo-Op1 presented the highest catalytic activity as a consequence of its higher amount of accessible Co^{3+} species in the Co_3O_4 crystal surface.

4. Conclusions

In summary, a conventional sol-gel one-pot methodology was described for the preparation of potential environmental Co-catalysts (10 wt.% of Co) supported on silica-titania using cobalt oxalate as the precursor salt for the formation of the Co_3O_4 active phase. The amount of Ti incorporated into the amorphous silica was varied (Si/Ti molar ratio of 5.7, 1.0 and 0.2) and the Co-catalysts evaluated in the CO oxidation between 100–550 °C (GHSV = 12,100 h^{-1}). SEM-EDS, TEM-EDS and TPR-H_2 results evidenced a higher and superficial cobalt dispersion in the one-pot prepared Co-catalysts when compared to the ones prepared by conventional impregnation with a cobalt nitrate solution. Furthermore, the simultaneous addition of cobalt oxalate during the incorporation by sol-gel of a controlled low Ti amount into the silica (nominal Si/Ti = 5.7, sample STCo-Op1) was determinant to improve the Co dispersion and to avoid the formation of Co-species with strong interaction with the support that consequently led to a CO oxidation Co-catalyst with the highest specific activity and, more importantly, having the lowest light-off temperature. As evidenced by XPS data, such Co-catalyst presented the highest superficial concentration of lattice O^{2-} and Co^{3+}, with these species playing an important role in the CO oxidation mechanism with O_2. On the other hand, Rietveld analyses, Raman spectroscopy and H_2-TPR data showed that the incorporation of a higher amount of Ti into the silica (more evident in the sample with Si/Ti nominal molar ratio of 0.2) led to the formation of Co_3O_4 and cobalt species with strong interaction with the support as cobalt titanate, which caused an increase in the Co reduction temperatures and, consequently decreasing the specific activity to CO oxidation. Coherently, the XPS spectrum of that sample showed lower concentration of lattice O^{2-} species and higher Co^{2+}/Co^{3+} ratio because of the parallel formation of cobalt titanate.

Acknowledgements

T. M. L. and W. N. C gratefully acknowledge CNPq and CAPES Brazilian Funding Agencies for the fellowships. The authors would also like to thank the Brazilian Petroleum Company (Petrobras) for the financial support.

Appendix A. Supplementary data

Supplementary material related to this article can be found, in the online version, at doi:https://doi.org/10.1016/j.apcata.2018.08.006.

References

[1] S. Royer, D. Duprez, ChemCatChem 3 (2011) 24–65.
[2] R. Wang, H. He, J. Wang, L. Liu, H. Dai, Catal. Today 201 (2013) 68–78.
[3] N. Kamiuchi, M. Haneda, M. Ozawa, Catal. Today 201 (2013) 79–84.
[4] W. Han, P. Zhang, Z. Tang, G. Lu, Process Saf. Environ. Prot. 92 (2014) 822–827.
[5] S. Salomons, R.E. Hayes, M. Votsmeier, A. Drochner, H. Vogel, S. Malmberg, J. Gieshoff, Appl. Catal. B Environ. 70 (2007) 305–313.
[6] S. Fuchs, T. Hahn, H.-G. Lintz, Chem. Eng. Process. Process Intensif. 33 (1994) 363–369.
[7] S.J.A. Figueroa, M.A. Newton, J. Catal. 312 (2014) 69–77.
[8] E. Alonso, F.R. Field, R.E. Kirchain, Environ. Sci. Technol. 46 (2012) 12986–12993.
[9] W. Liu, M. Flytzani-stephanopoulos, Chem. Eng. J. 64 (1996) 283–294.
[10] A. Biabani-Ravandi, M. Rezaei, Z. Fattah, Process Saf. Environ. Prot. 91 (2013) 489–494.
[11] I.V. Lukiyanchuk, V.S. Rudnev, I.V. Chernykh, I.V. Malyshev, L.M. Tyrina, M.V. Adigamova, Surf. Coat. Technol. 231 (2013) 433–438.
[12] M. Kang, M.W. Song, C.H. Lee, Appl. Catal. A Gen. 251 (2003) 143–156.
[13] H. Lin, H. Chiu, H. Tsai, S. Chien, C. Wang, Catal. Lett. 88 (2003) 169–174.
[14] J. Jansson, M. Skoglundh, E. Fridell, P. Thormählen, Top. Catal. 2 (2001) 385–389.
[15] Y. Lou, J. Ma, X. Cao, L. Wang, Q. Dai, Z. Zhao, Y. Cai, W. Zhan, Y. Guo, P. Hu, G. Lu, Y. Guo, ACS Catal. 4 (2014) 4143–4152.
[16] H. Wu, Y. Yang, H. Suo, M. Qing, L. Yan, B. Wu, J. Xu, H. Xiang, Y. Li, J. Mol. Catal. A Chem. 390 (2014) 52–62.
[17] Y. Yu, T. Takei, H. Ohashi, H. He, X. Zhang, M. Haruta, J. Catal. 267 (2009) 121–128.
[18] J. Jansson, A.E.C. Palmqvist, E. Fridell, M. Skoglundh, L. Osterlund, P. Thormahlen, V. Langer, J. Catal. 211 (2002) 387–397.
[19] X. Xie, Y. Li, Z. Liu, M. Haruta, W. Shen, Nature 458 (2009) 746–749.
[20] G. Salek, P. Alphonse, P. Dufour, S. Guillemet-Fritsch, C. Tenailleau, Appl. Catal. B Environ. 147 (2014) 1–7.
[21] D. Gu, C.J. Jia, C. Weidenthaler, H.J. Bongard, B. Spliethoff, W. Schmidt, F. Schüth, J. Am. Chem. Soc. 137 (2015) 11407–11418.
[22] J. Regalbuto, Catalyst Preparation - Science and Engineering, CRC PRess, 2007.
[23] R.J. Davis, Z. Liu, Chem. Mater. 4756 (1997) 2311–2324.
[24] E.I. Ko, J. Chen, J.G. Weissman, J. Catal. 520 (1987) 511–520.
[25] R. Jin, Z. Wu, Y. Liu, B. Jiang, H. Wang, J. Hazard. Mater. 161 (2009) 42–48.
[26] K.M.S. Khalil, A.A. Elsamahy, M.S. Elanany, J. Colloid Interface Sci. 249 (2002) 359–365.
[27] Y. Hayashi, Chem. Sci. 7 (2016) 866–880.
[28] H.N. Wang, P. Yuan, L. Zhou, Y.N. Guo, J. Zou, A.M. Yu, G.Q. Lu, C.Z. Yu, J. Mater. Sci. 44 (2009) 6484–6489.
[29] Y.J. Lin, Y.H. Chang, W.D. Yang, B.S. Tsai, J. Non. Solids 352 (2006) 789–794.
[30] K. Takanabe, K. Nagaoka, K. Nariai, K. Aika, J. Catal. 232 (2005) 268–275.
[31] K.J.A. Raj, M.G. Prakash, T. Elangovan, B. Viswanathan, Catal. Lett. 142 (2012) 87–94.
[32] B. Jongsomjit, C. Sakdamnuson, J.G. Goodwin Jr, P. Praserthdam, Catal. Lett. 94 (2004) 209–215.
[33] K. Suriye, P. Praserthdam, B. Jongsomjit, Catal. Commun. 8 (2007) 1772–1780.
[34] W.H. Yang, M.H. Kim, S.W. Ham, Catal. Today 123 (2007) 94–103.
[35] V. Iablokov, R. Barbosa, G. Pollefeyt, I. Van Driessche, S. Chenakin, N. Kruse, ACS Catal. 5 (2015) 5714–5718.
[36] I. Puskas, T.H. Fleisch, J.A. Kaduk, C.L. Marshall, B.L. Meyers, M.J. Castagnola, J.E. Indacochea, Appl. Catal. A Gen. 316 (2007) 197–206.
[37] I. Puskas, T.H. Fleisch, P.R. Full, J.A. Kaduk, C.L. Marshall, B.L. Meyers, Appl. Catal. A Gen. 311 (2006) 146–154.
[38] Y. Brik, M. Kacimi, M. Ziyad, J. Catal. 128 (2001) 118–128.
[39] S.J. Gregg, K.S.W. Sing, Adsorption, Surface Area and Porosity, Academic Press, 1982.
[40] S. Klein, B.M. Weckhuysen, J.A. Martens, W.F. Maier, P.A. Jacobs, J. Catal. 491 (1996) 489–491.
[41] V. Lafond, P.H. Mutin, A. Vioux, Chem. Mater. 16 (2004) 5380–5386.
[42] M. Voß, D. Borgmann, G. Wedler, J. Catal. 212 (2002) 10–21.
[43] M.M. Yung, E.M. Holmgreen, U.S. Ozkan, J. Catal. 247 (2007) 356–367.
[44] S. Storsæter, B. Tøtdal, J.C. Walmsley, B. Steinar, A. Holmen, J. Catal. 236 (2005) 139–152.
[45] P.M. Sreekanth, Æ.P.G. Smirniotis, Catal. Lett. 122 (2008) 37–42.
[46] X. Zhang, F. Zhang, K.Y. Chan, Appl. Catal. A Gen. 284 (2005) 193–198.
[47] G. Xu, Z. Zheng, Y. Wu, N. Feng, Ceram. Int. 35 (2009) 1–5.
[48] C. He, B. Tian, J. Zhang, J. Colloid Interface Sci. 344 (2010) 382–389.
[49] C. Ren, W. Qiu, Y. Chen, Sep. Purif. Technol. 107 (2013) 264–272.
[50] S.G. Christoskova, M. Stoyanova, M. Georgieva, D. Mehandjiev, Mater. Chem. Phys. 60 (1999) 39–43.
[51] C.W. Tang, C.B. Wang, S.H. Chien, Thermochim. Acta 473 (2008) 68–73.
[52] M.A. Gabal, S.A. Hameed, A.Y. Obaid, Mater. Charact. 71 (2012) 87–94.
[53] X. Wang, J. Shen, Q. Pan, J. Raman Spectrosc. 42 (2011) 1578–1582.
[54] Y.K. Sharma, M. Kharkwal, S. Uma, R. Nagarajan, Polyhedron 28 (2009) 579–585.
[55] M.I. Baraton, G. Busca, M.C. Prieto, G. Ricchiardi, V.S. Escribano, J. Solid State Chem. 112 (1994) 9–14.

[56] T. Xiao, S. Ji, H. Wang, K.S. Coleman, M.L. Green, J. Mol. Catal. A Chem. 175 (2001) 111–123.
[57] R.C. Pedroza, S.W. da Silva, M.A.G. Soler, P.P.C. Sartoratto, D.R. Rezende, P.C. Morais, J. Magn. Magn. Mater. 289 (2005) 139–141.
[58] C.X. Liu, Q. Liu, X.G. Huang, X. Nie, Z. Huang, J. Chin. Chem. Soc. 61 (2014) 490–494.
[59] Z. Chen, C.X. Kronawitter, B.E. Koel, Phys. Chem. Chem. Phys. 17 (2015) 29387–29393.
[60] J.L. Gautier, E. Rios, M. Gracia, J.F. Marco, J.R. Gancedo, Thin Solid Films 311 (1997) 51–57.
[61] X. Tang, F. Gao, Y. Xiang, H. Yi, S. Zhao, X. Liu, Y. Li, Ind. Eng. Chem. Res. 54 (2015) 9116–9123.
[62] S. Todorova, H. Kolev, J.P. Holgado, G. Kadinov, C. Bonev, R. Pereñíguez, A. Caballero, Appl. Catal. B Environ. 94 (2010) 46–54.
[63] D. Enache, M. Roy-Auberger, R. Revel, Appl. Catal. A Gen. 268 (2004) 51–60.
[64] I. Arvanitidis, A. Kapilashrami, D. Sichen, S. Seetharaman, J. Mater. Res. 15 (2000) 338–346.
[65] Y. Liu, I. Florea, O. Ersen, C. Pham-Huu, C. Meny, Chem. Commun. (Camb.) 51 (2014) 145–148.
[66] M.Y. Kim, Y.S. You, H.S. Han, G. Seo, Catal. Lett. 120 (2007) 40–47.
[67] H. Li, J. Li, H. Ni, D. Song, Catal. Letters 110 (2006) 71–76.
[68] J. Jansson, J. Catal. 194 (2000) 55–60.
[69] P. Broqvist, I. Panas, H. Persson, J. Catal. 210 (2002) 198–206.
[70] S. Lv, G. Xia, C. Jin, C. Hao, L. Wang, J. Li, Y. Zhang, J.J. Zhu, Catal. Commun. 86 (2016) 100–103.
[71] Y. Lou, L. Wang, Z. Zhao, Y. Zhang, Z. Zhang, G. Lu, Y. Guo, Y. Guo, Appl. Catal. B Environ. 146 (2014) 43–49.
[72] F. Wang, L. Zhang, L. Xu, Z. Deng, W. Shi, Fuel 203 (2017) 419–429.
[73] L. Hu, K. Sun, Q. Peng, B. Xu, Y. Li, Nano Res. 3 (2010) 363–368.
[74] X. Xie, W. Shen, Nanoscale 1 (2009) 50–60.
[75] S.A. Singh, G. Madras, Appl. Catal. A Gen. 504 (2015) 463–475.
[76] X.Y. Pang, C. Liu, D.C. Li, C.Q. Lv, G.C. Wang, ChemPhysChem 14 (2013) 204–212.
[77] X. Jiang, G. Ding, L. Lou, Y. Chen, X. Zheng, Catal. Today 93–95 (2004) 811–818.